Downward continuation with explicit extrapolators and common-azimuth migration

*Eric Dussaud**

ABSTRACT

We present a review of explicit extrapolation schemes in the context of 3-D poststack migration, and demonstrate why these methods are appealing when strong lateral velocity variations are present. The 3-D wavefield depth extrapolation is implemented by means of short 1-D spatial convolution operators in combination with McClellan transformation filters which are used to turn 1-D finite impulse response filters into 2-D filters. The 1-D convolution operators are designed by using either a weighted least-squares method, a truncated Taylor expansion, or the Remez algorithm. McClellan transformation filters are extended to accomodate unequal in-line and cross-line sampling intervals. We also present an attempt at using an explicit scheme for prestack migration of common-offset data under the common azimuth assumption. Preliminary results are encouraging and suggest that these schemes may prove useful. This remains to be further investigated.

INTRODUCTION

Explicit space-frequency domain extrapolation schemes have gained a wide acceptance over the last decade. For poststack migration, these methods are based on the approximation of the single square root operator with a finite-length 2-D convolutional filter in the space domain [1; 13; 5]. Because downward continuation is performed via convolutions in the space domain, the coefficients of the depth extrapolation filter may vary as a function of spatial location. Therefore, explicit schemes can in principle accomodate strong lateral velocity contrasts in the medium, with no additional computational cost.

To reduce the computational cost associated with the application of 2-D convolution filters, and to simplify the design of the continuation operator, one can exploit the circular symmetry of the operator and break the design procedure into two parts [10; 11]. The first

*The Rice Inversion Project, Department of Computational and Applied Mathematics, Rice University, Houston, TX 77005-1892 USA, email dussaud@caam.rice.edu

part involves the computation of the coefficients of 1-D extrapolation filters that would be used for 2-D migration. The second part involves the computation of a small transformation filter that, when applied in conjunction with the Chebyshev recursion, gives nearly circular symmetry. Because downward continuation is done recursively, stability of the explicit schemes is a key component in the design of the both the coefficients and the transformation filters. Special care must be taken to ensure that evanescent waves and waves propagating at angles higher than the maximum design angle are prevented from growing exponentially. Several methods have been proposed to perform these two tasks. In this paper, we give only an overview of three different techniques used to compute the 1D coefficients as well as a description of two different transformation filters. We further describe how the transformation filter can be modified to take into account unequal in-line and cross-line sampling intervals. We also show how the Li correction [15; 8] can be used to correct some of the errors associated with the filter. Finally, we present a way to perform common-azimuth prestack migration of common-offset data using an innovative explicit scheme.

DESIGN OF 1-D CONVOLUTION OPERATORS

The 2-D extrapolation operator has the form

$$W(k_x, \Delta z, \omega) \equiv \exp\left[i\Delta z \sqrt{\frac{\omega^2}{v^2} - k_x^2} \right] \tag{1}$$

The objective is to obtain 1D short convolution operators $f(x, \Delta z, \omega)$ with complex coefficients f_n that are function of Δz, ω, and v, and with a wavenumber spectrum $F(k_x, \Delta z, \omega)$ which approximates the original phase shift operator (1) over a desired wavenumber band. Because the exact operator is symmetric with respect to $k_x = 0$, the inverse Fourier transform of $f(x, \Delta z, \omega)$ over the wavenumber k_x takes the form:

$$F(k_x, \Delta z, \omega) \approx f_0 + 2 \sum_{n=1}^{(N-1)/2} f_n \cos(n\Delta x k_x). \tag{2}$$

The symmetry implies that the complex coefficients f_n are even (both real and imaginary parts), so that the total number of coefficients N is odd. Note that the filter is uniquely determined by $(N+1)/2$ coefficients.

The design can be realized by using a method based on a truncated Taylor series expansion of both the extrapolation operator and its aproximation [10]. The idea is to match the coefficients of the terms in each series at $k_x = 0$. Because a direct match of all the coefficients in the Taylor series would result in a response $F(k_x)$ with $|F(k_x)| > 1$ beyond a certain wavenumber k_x, violating the stability constraint, Hale suggested to match only the first M terms in the series and set the remaining $M - N$ to 0. We refer the reader to [11] for a more detailed description.

Because the error associated with the Taylor expansion is unnecessarily small for small k_x, and grows rapidly with increasing k_x, alternative techniques have posed the design problem as a constrained optimization problem: the objective is to determine the filter coefficients f_n such that:

$$\sum_k \left\| \phi \left[F(k_x, \Delta z, \omega) - W(k_x, \Delta z, \omega) \right] \right\| \tag{3}$$

is minimized, with the constraint:

$$\left| F(k_x, \Delta z, \omega) \right| < 1 \quad \text{for } k_c < k_x < k_{\text{NYQ}}.$$

Here $\phi \equiv \phi(k_x)$ is a positive weighting function. The wavenumbers k_c and k_{NYQ} are the critical and Nyquist wavenumbers, respectively:

$$k_c = \frac{\omega}{v} \sin \alpha_{\max}, \qquad k_{\text{NYQ}} = \frac{\pi}{\Delta x},$$

where $\alpha_{\max}$ is the maximum dip to be accurately migrated. With the choice of the L_∞ norm, the optimization problem (3) can be solved using the Remez algorithm [17; 22]. Both real and imaginary part of the extrapolation operator are optimized in the L_∞ norm (the Remez algorithm operates on real functions), which guarantees both accuracy and stability [22]. Furthermore, the theory of Chebyshev approximation has established that the problem as formulated in (3) has a unique solution. Necessary and sufficient conditions characterizing the best approximation are given by the alternation theorem [6].

The weighted least-squares method [23; 24; 25; 26], thereby using the L_2 norm, provides an interesting alternative. The optimization problem becomes that of determining the operators f that minimize

$$\tfrac{1}{2} \left\| \Lambda^{1/2} \left[\Gamma f(\Delta x, \Delta z, \omega) - F(\Delta k_x, \Delta z, \omega) \right] \right\|_2^2 .$$

Here Λ is a diagonal weighting matrix, and Γ represents the Fourier transform matrix. The least-squares solution is given by

$$f(\Delta x, \Delta z, \omega) = \left[\Gamma^T \Lambda \Gamma \right]^{-1} \Gamma^T \Lambda F(\Delta k_x, \Delta z, \omega)$$

All three methods have been implemented and tested with JavaSeis, the seismic migration software used within HGRG. All three methods provide reliable coefficients. Some comparison results and comments may be found in [7].

TRANSFORMATION FILTERS

The McClellan transformation [16] has been widely used to turn 1-D finite impulse response filters into 2-D filters. To design 2-D extrapolation filters, Hale [10] proposed to use the circular symmetry of the 2-D extrapolation operator to write:

$$W(k_x, k_y, \Delta z, \omega) \approx w_0 + 2 \sum_{n=1}^{(N-1)/2} w_n \cos(n \Delta x k_r), \tag{4}$$

with $k_r = \sqrt{k_x^2 + k_y^2}$. The filters $\cos(n\Delta x k_r)$ are expensive to apply because their length grows linearly with n. Fortunately, they can be derived from the $\cos(\Delta x k_r)$ filter by the Chebyshev recursion formula [10]. To approximate the latter, Hale [10] suggested the following *improved* McClellan transform:

$$\begin{aligned}\cos(\Delta x k_r) \approx G(k_x, k_y) \equiv & \\ & -1 + \frac{1}{2}\left[1 + \cos(\Delta x k_x)\right]\left[1 + \cos(\Delta x k_y)\right] \\ & -\frac{c}{2}\left[1 - \cos(2\Delta x k_x)\right]\left[1 - \cos(2\Delta x k_y)\right]\end{aligned} \tag{5}$$

with $c = 0.0255$. We denote by $g(x, y)$ the corresponding 5x5 spatial stencil (obtained by inverse Fourier transform):

$$g(x,y) \equiv \begin{bmatrix} -c/8 & 0 & c/4 & 0 & -c/8 \\ 0 & 1/8 & 1/4 & 1/8 & 0 \\ c/4 & 1/4 & -(1+c)/2 & 1/4 & c/4 \\ 0 & 1/8 & 1/4 & 1/8 & 0 \\ -c/8 & 0 & c/4 & 0 & -c/8 \end{bmatrix}$$

The 2-D inverse Fourier transform of (4) is given by:

$$w(x, y, \Delta z, \omega) = w_0 \delta(x, y) + 2 \sum_{n=1}^{N} w_n g_n(x, y), \tag{6}$$

where $g_0 \equiv \delta(x, y)$, $g_1 \equiv g$ and the operators g_n, $n > 1$ are obtained from g with the Chebyshev recursion formula. The extrapolation step simply consists of convolving the wavefield at depth z with (6).

The accuracy of migration methods based on McClellan transformations depends on how well the filter $\cos(\Delta x k_r)$ is approximated. Errors in this approximation cause anisotropy in the extrapolation operator and frequency dispersion in the migrated results [2]. Several enhancements have been proposed and investigated [4; 9; 2; 19; 18]. Alternative approximations of the $\cos(\Delta x k_r)$ filter have also been proposed [22; 21]. As an example, we present here the transformation set forth by Hazra and Reddy [12; 20] and discussed in [19]. Their scaled and shifted approximation is given by:

$$\begin{aligned}\cos(\Delta x k_r) \approx & -\frac{g}{2} + \frac{g}{2}\cos(\Delta x k_x) + \frac{g}{2}\cos(\Delta x k_y) \\ & + \left[1 - \frac{g}{2}\right]\cos(\Delta x k_x)\cos(\Delta x k_y)\end{aligned} \tag{7}$$

where g is a function of the critical wavenumber k_x^c of the 2-D extrapolation filter along the in-line direction. Figure 1 displays the contours of constant amplitude and phase for the scaled and shifted Hazra & Reddy transformation with $k_x^c = k_{\text{NYQ}}$ and for the improved McClellan transformation. The approximation (7) is clearly better for wavenumbers closer to the Nyquist wavenumber. The inverse Fourier transform of (7) is a 3x3 stencil, hence much cheaper to apply than the transform proposed by Hale. Practical issues regarding implementation details can be found in [19; 23].

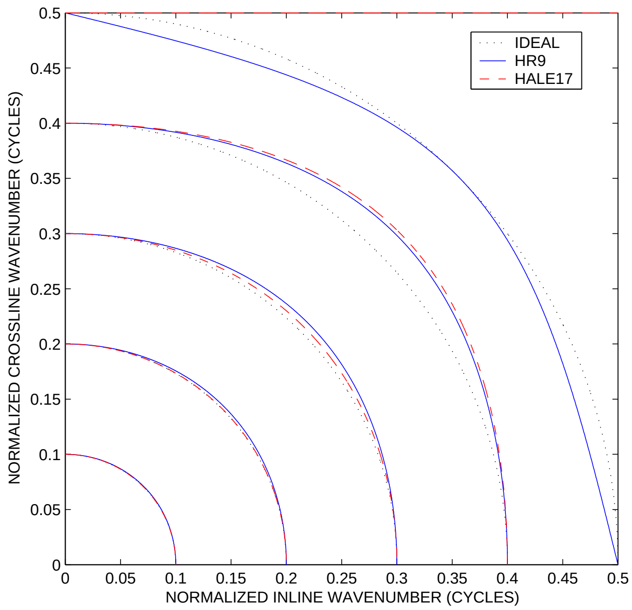

FIG. 1. Contours of constant amplitude and phase for the scaled and shifted Hazra & Reddy transformation compared to the improved McClellan transformation and the ideal circular response.

EXTENSION OF UNEQUAL SAMPLING INTERVALS

We follow the method proposed by Levin [14] for extending Hale's transformation filter to handle surveys binned and stacked with different in-line and cross-line intervals. The transformation of Hazra and Reddy can be extended in a similar way [27]. The key idea is to use dispersion relations for finite-difference schemes.

Define $\hat{k}_x$ by the second difference operator:

$$\frac{\delta^2 p}{\delta x^2} = \frac{p(x+\Delta x) - 2p(x) + p(x-\Delta x)}{(\Delta x)^2} \Longleftrightarrow -\hat{k}_x^2 P \tag{8}$$

Inserting the harmonic $e^{ik_x x}$ in (8) yields:

$$\cos(\Delta x k_x) = 1 - \frac{(\Delta x)^2}{2}\hat{k}_x^2 \Longleftrightarrow \begin{bmatrix} \frac{1}{2} & 0 & \frac{1}{2} \end{bmatrix} \tag{9}$$

Therefore, setting $\gamma \equiv (\Delta x/\Delta y)^2$, we obtain:

$$\cos(\Delta x k_y) = 1 - \frac{(\Delta x)^2}{2}\hat{k}_y^2 \Longleftrightarrow \begin{bmatrix} \gamma/2 & (1-\gamma) & \gamma/2 \end{bmatrix},$$

A similar argument can be made to connect the filter $cos(2\Delta x k_x)$ to a linear combination of both second and fourth finite difference operators [7]:

$$\cos(2\Delta x k_x) = -\tfrac{1}{2}(\Delta x)^4 \hat{k_x}^4 - 2(\Delta x)^2 \hat{k_x}^2 + 1,$$

where $\hat{k_x}^4$ denotes the fourth finite difference approximation. Therefore:

$$\begin{aligned}\cos(2k_y\Delta x) &= -\tfrac{1}{2}\hat{k_y}^4(\Delta x)^4 - 2(\Delta x)^2\hat{k_y}^2 + 1 \\ &\Longleftrightarrow \begin{bmatrix}\frac{\gamma^2}{2} & 2\gamma(1-\gamma) & 3\gamma^2-4\gamma+1 & 2\gamma(1-\gamma) & \frac{\gamma^2}{2}\end{bmatrix},\end{aligned}$$

where γ is the ratio of sampling intervals defined above. The resulting stencil (obtained by inverse Fourier transform) is given by:

$$\frac{1}{2}\begin{bmatrix} -c\gamma^2/4 & -c\gamma(1-\gamma) & -c\gamma(3\gamma-4)/2 & -c\gamma(1-\gamma) & -c\gamma^2/4 \\ 0 & \gamma/4 & 1-\gamma/2 & \gamma/4 & 0 \\ c\gamma^2/2 & 2c\gamma(1-\gamma)+\gamma/2 & -\gamma-c\gamma(3\gamma-4) & 2c\gamma(1-\gamma)+\gamma/2 & c\gamma^2/2 \\ 0 & \gamma/4 & 1-\gamma/2 & \gamma/4 & 0 \\ -c\gamma^2/4 & -c\gamma(1-\gamma) & -c\gamma(3\gamma-4)/2 & -c\gamma(1-\gamma) & -c\gamma^2/4 \end{bmatrix}$$

It has 21 non-zero terms, resulting in an increase of about 25% compared to the original transformation [14]. It is symmetric vertically and horizontally, but not symmetric under transposition, except when $\gamma = 1$, which is precisely the case when the in-line and cross-line spacings are identical. We tested this transformation filter on a synthetic data set created with a velocity model containing very strong lateral velocity contrasts (the velocity ranges from 1.5km/s to 7km/s). Figure 2 (top panel) shows the velocity model as well as the position of the reflectors. The data set (Figure 2, bottom panel) consists of 101 cross-lines with a spacing of 40m, and 401 in-lines with a spacing of 25m. The result obtained using a convolution operator with 39 coefficients along with Hale's improved transform (Figure 4, top panel) is nearly perfect. However, the same vertical slice obtained with the JavaSeis hybrid screen propagator (Figure 4, bottom panel) shows that the middle portion of top reflector is inaccurately imaged. This example demonstrates the limitations of implicit methods in the presence of strong lateral velocity variations.

LI CORRECTION FOR EXPLICIT METHODS

Li's correction, originally designed to compensate errors associated with the splitting approximation used in implicit schemes, has been extended in a straightforward way to explicit depth extrapolation methods [8]. Using equation (5), we define $\hat{k}_r$ by:

$$\hat{k}_r = \frac{1}{\Delta x}\cos^{-1}\left[G(k_x, k_y)\right].$$

The error that accumulates during the recursive depth extrapolation due to the approximation (5) is clearly due to the difference between k_r and $\hat{k}_r$. Expressed in the wavenumber domain for the constant velocity case, the error after n extrapolation steps is:

$$E(k_x, k_y, \omega) = \exp\left[in\Delta z\left(\sqrt{\frac{\omega^2}{v^2} - \hat{k}_r^2} - \sqrt{\frac{\omega^2}{v^2} - k_r^2}\right)\right]$$

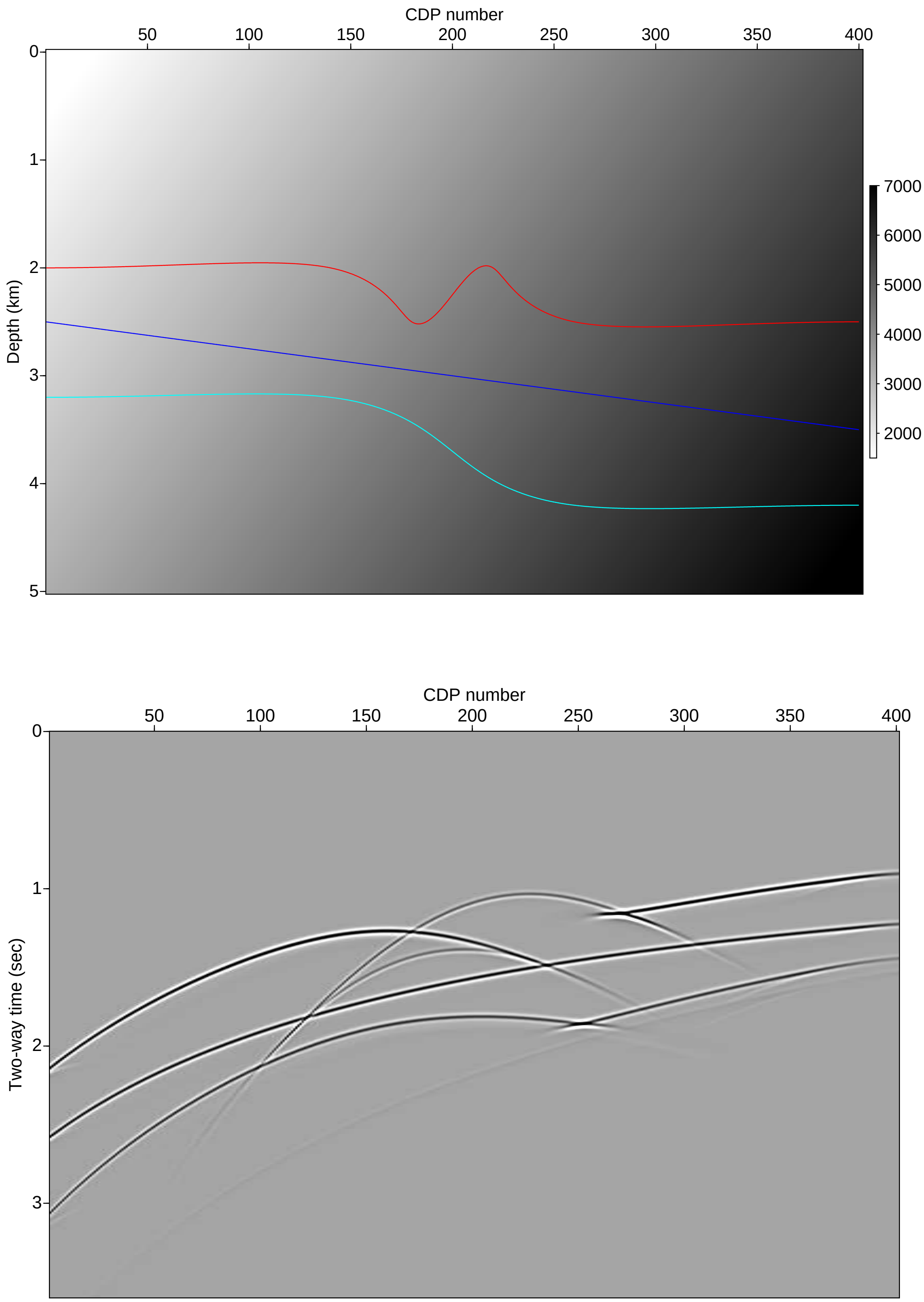

FIG. 2. Top: velocity section at $y = 0$; reflectivity model is overlaid. Bottom: section of the synthetic data at $y = 0$.

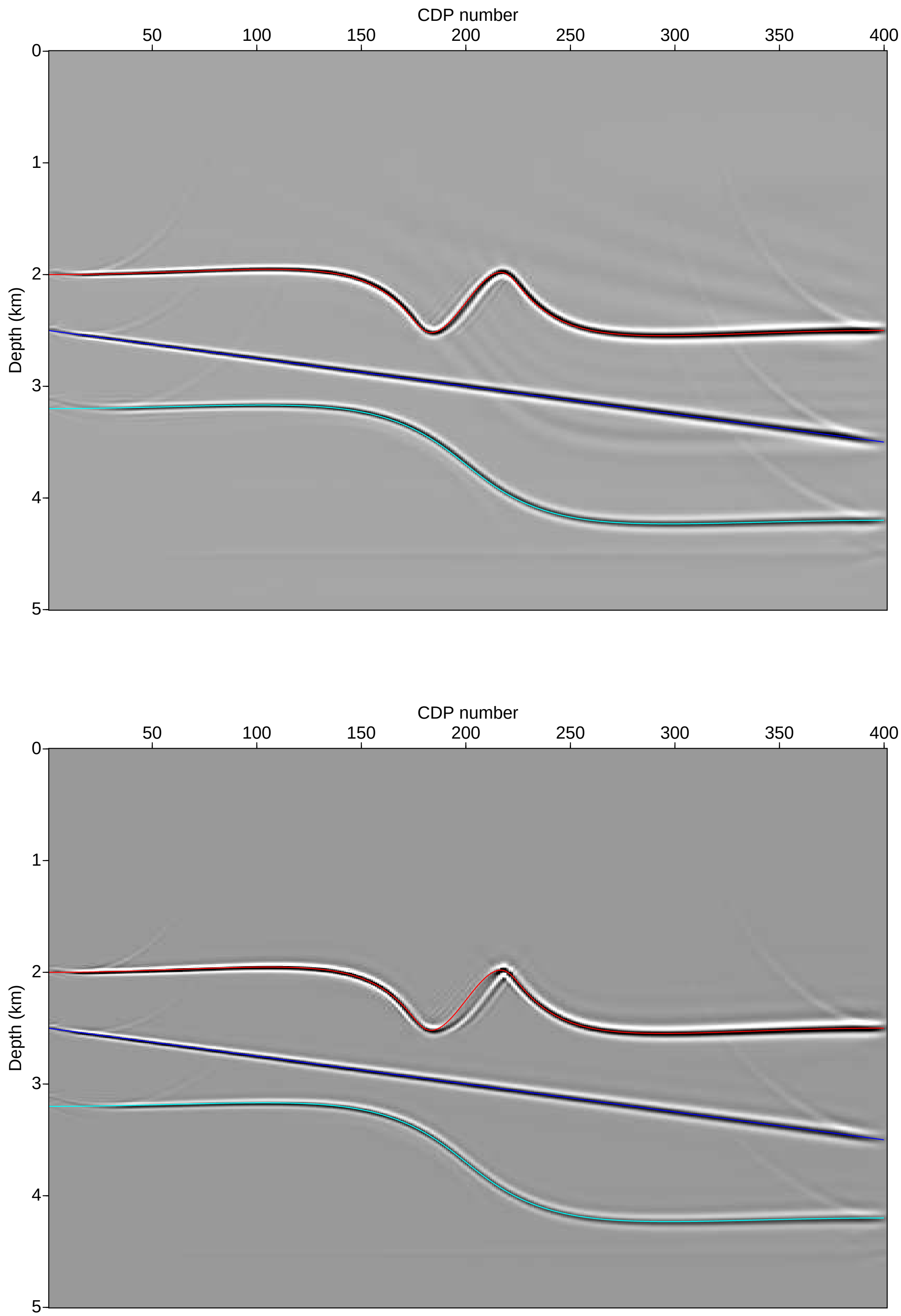

Fig. 3. In-line section at $y = 0$ in the migrated cube obtained with the explicit propagator (top) and the hybrid screen propagator (bottom).

To handle lateral velocity variations, Etgen and Nichols [8] suggest to remove phase errors due to the McClellan transform for a single reference velocity $v = v_0$ in the above expression. That reference velocity could be, for instance, the average over n depth slabs of the minimum velocity in each depth slice, i.e.

$$v_0 = \frac{1}{n} \sum_{k=0}^{n-1} \min_{x,y} v(x, y, z + k\Delta z)$$

Note that in the case of strong lateral velocity variations, it may be necessary to perform the Li correction for several reference velocities, similar to the phase-shift plus interpolation method. In practice, the Li correction is applied to the wavefield after n extrapolation depths by simple multiplication in the wavenumber domain:

$$P(k_x, k_y, \omega) \leftarrow \overline{E(k_x, k_y, \omega, v_0)} P(k_x, k_y, \omega)$$

Figure 4 shows a vertical slice of an impulse response in a two-velocity medium using Hale's improved transform (top panel) and the same slice obtained using the same transform and with the Li correction applied every 10 extrapolation steps (bottom panel). The Li-corrected impulse response clearly shows less frequency dispersion compared to the original migration result. It is also closer to have the correct shape.

As pointed out by Etgen and Nichols [8], this approach is general, and could be extended to compensate for other sources of error, such as those due to the truncation of the discrete Fourier transform (2) in the design of the 1-D coefficients. This remains to be further investigated.

COMPARISON WITH A WELL-TUNED IMPLICIT SCHEME

We compared the results of zero-offset migration obtained using an explicit operator designed with 39 coefficients and with the improved McClellan transformation filter (with Li's correction every 16 extrapolation steps) with those obtained with the JavaSeis hybrid screen propagator (with dip filtering at every step) on the so-called **steep model**, a synthetic data set created at the Institut Francais du Petrole (IFP) containing both very steep reflectors (with dips up to 72 degrees) and strong lateral velocity variations. The data consists of 256 in-lines and cross-lines, with a spacing of 20m in both directions.

Figures 5 displays a vertical slice through the velocity model at $y = 0$ (top panel) and along the $x = y$ direction (bottom panel), respectively. The corresponding migration results are shown on Figures 6 and 7. The results obtained using the hybrid screen method (bottom panels) are overall cleaner and sharper. By contrast, the migration results obtained using the McClellan migration scheme (top panels) contain more frequency dispersion. However, the leftmost part of the bottom reflector is in both sections better imaged by the explicit scheme. Moreover, the artifacts caused by splitting present in the 45^o-azimuth section obtained using the hybrid screen method are not visible in the image obtained by the

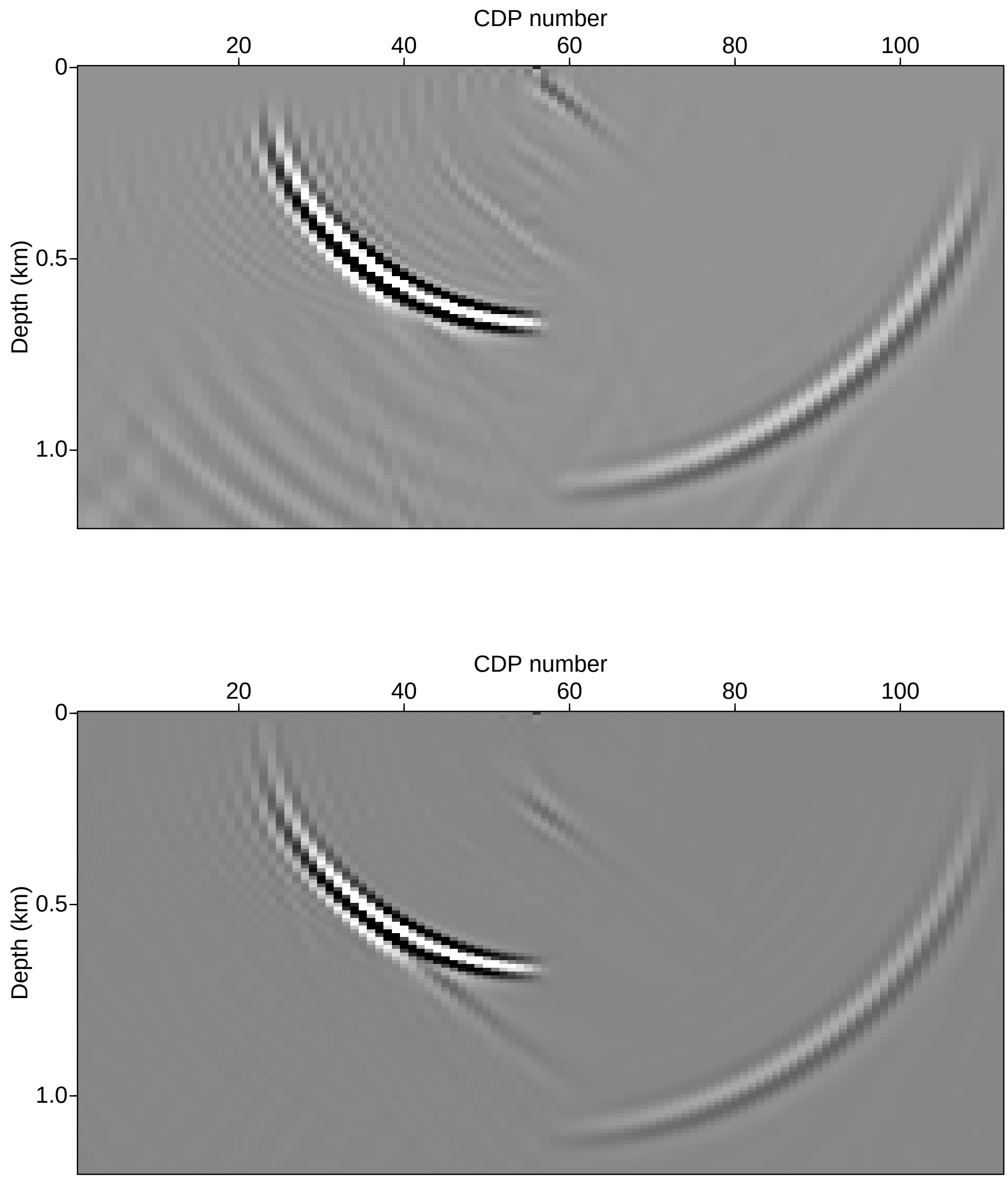

FIG. 4. Effect of the Li correction on the 3-D migration of an impulse response with an operator of 25 spatial points designed using weighted least-squares

explicit scheme. These preliminary results are satisfactory. Several improvements can still be made to enhance the quality obtained with the explicit scheme, namely in the design of the 1-D coefficients, in the design of more accurate transformation filters, as well as in the design of more elaborate correction filters.

COMMON-AZIMUTH MIGRATION

In this section, we present an attempt at using explicit methods for the migration of common-offset, common-azimuth data [3]. After approximation with splitting, the dispersion relation associated with common-azimuth downward continuation is given by:

$$\widehat{k_z} = k_{z_x} + \sqrt{\frac{4\omega^2}{v_m^2} - k_{m_y}^2} - \frac{2\omega}{v_m}, \tag{10}$$

where:

$$k_{z_x} = \sqrt{\frac{\omega^2}{v_s^2} - \frac{1}{4}\left(k_{m_x} - k_{h_x}\right)^2} + \sqrt{\frac{\omega^2}{v_g^2} - \frac{1}{4}\left(k_{m_x} + k_{h_x}\right)^2}$$

With this approximation, common-azimuth migration is applied in two steps: first as a convolution operator along the in-line direction, and then as convolution operator along the cross-line direction. Short convolution operators can be designed in the usual way to approximate each of the three extrapolation operators:

$$D_1(k_{m_x}, k_{h_x}, \Delta z, \omega) = \exp\left[i\Delta z\sqrt{\frac{\omega^2}{v_s^2} - \frac{1}{4}\left(k_{m_x} - k_{h_x}\right)^2}\right]$$

$$D_2(k_{m_x}, k_{h_x}, \Delta z, \omega) = \exp\left[i\Delta z\sqrt{\frac{\omega^2}{v_g^2} - \frac{1}{4}\left(k_{m_x} + k_{h_x}\right)^2}\right]$$

$$D_3(k_{m_y}, \Delta z, \omega) = \exp\left[i\Delta z\sqrt{\frac{4\omega^2}{v_m^2} - k_{m_y}^2} - \frac{2\omega}{v_m}\right]$$

The convolution operator in the cross-line direction is one-dimensional, and is therefore both trivial to design and implement. On the other hand, the convolution operators along the in-line direction require special care. In order to highlight some of the implementation details, we describe more precisely the design of the operator D_1. Setting $k_s = k_{m_x} - k_{h_x}$, we rewrite this operator as:

$$D_1(k_{m_x}, k_{h_x}, \Delta z, \omega) = \exp\left[i\frac{\Delta z}{2}\sqrt{\frac{4\omega^2}{v_s^2} - k_s^2}\right].$$

It can be approximated by the finite-length summation:

$$D_1(k_{m_x}, k_{h_x}, \Delta z, \omega) \approx d_0 + 2\sum_{n=1}^{N_h-1} d_n \cos(n\Delta x k_s), \tag{11}$$

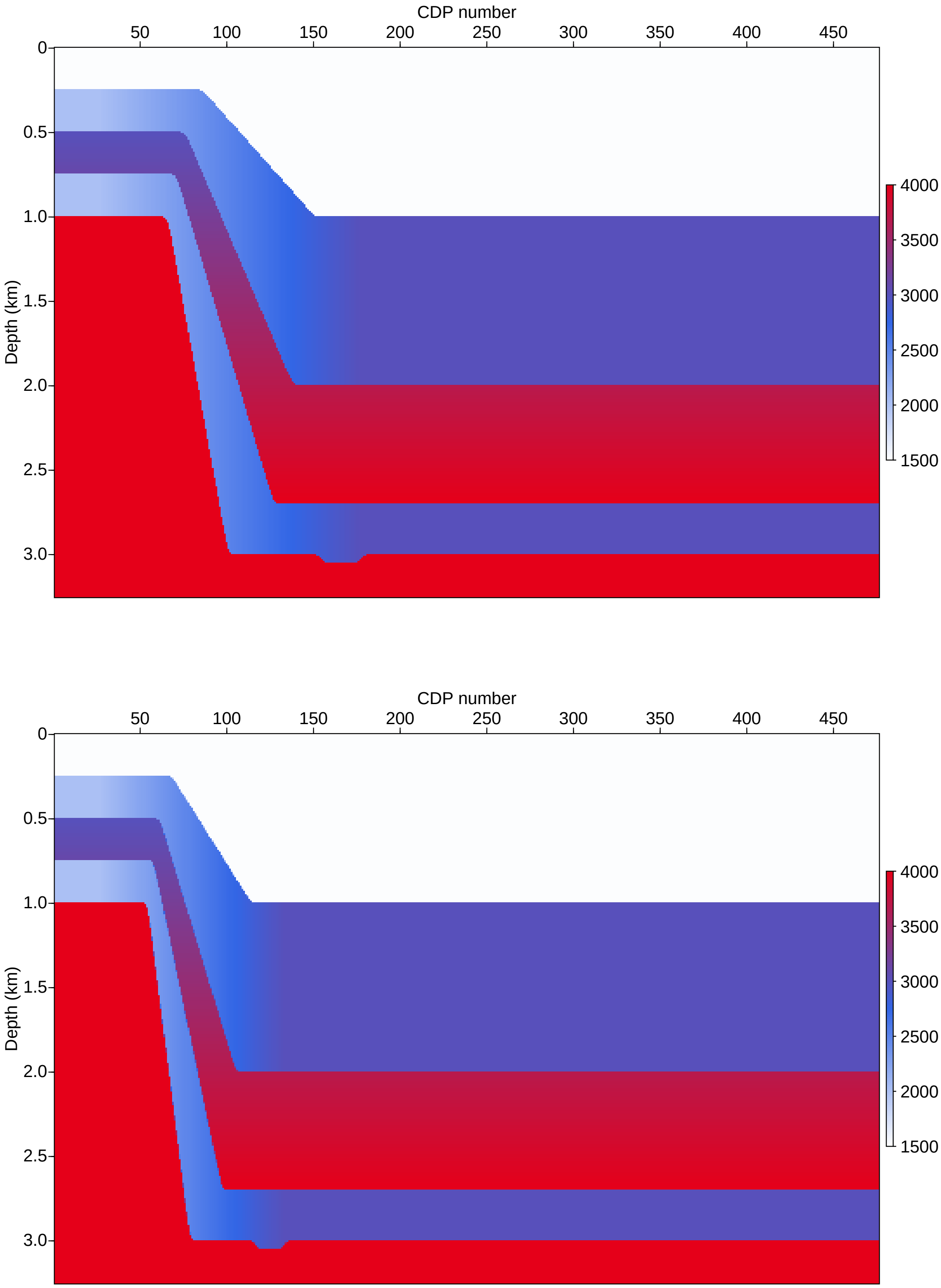

FIG. 5. Top: velocity section at $y = 0$. Bottom: velocity section along $x = y$.

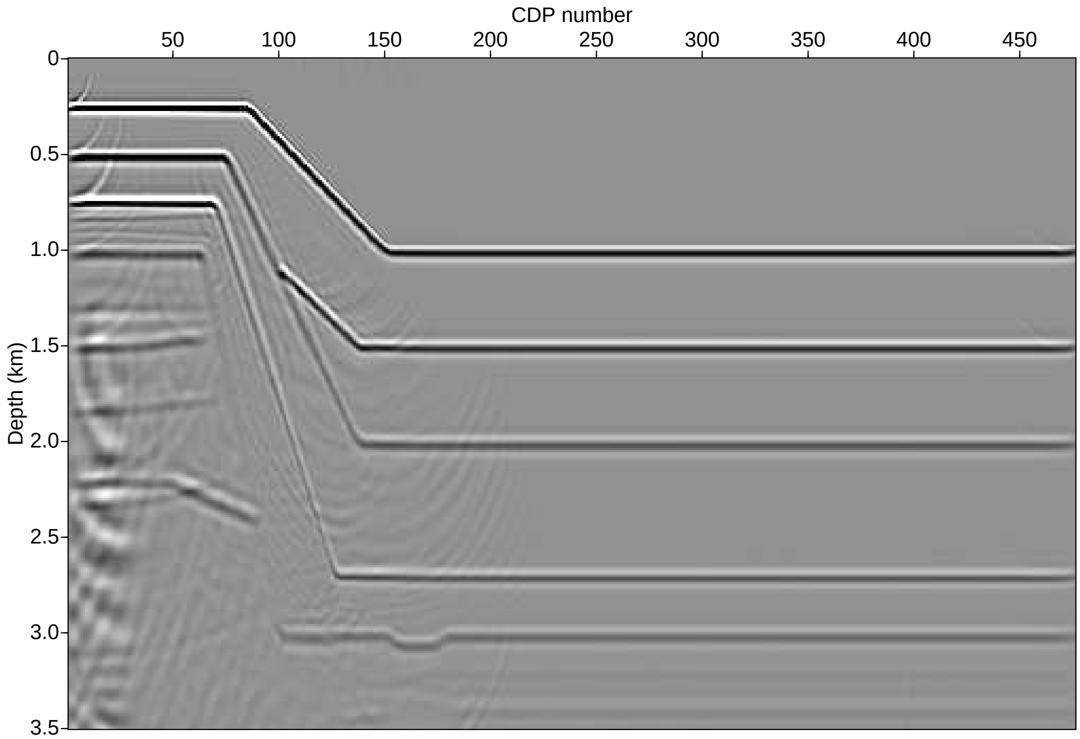

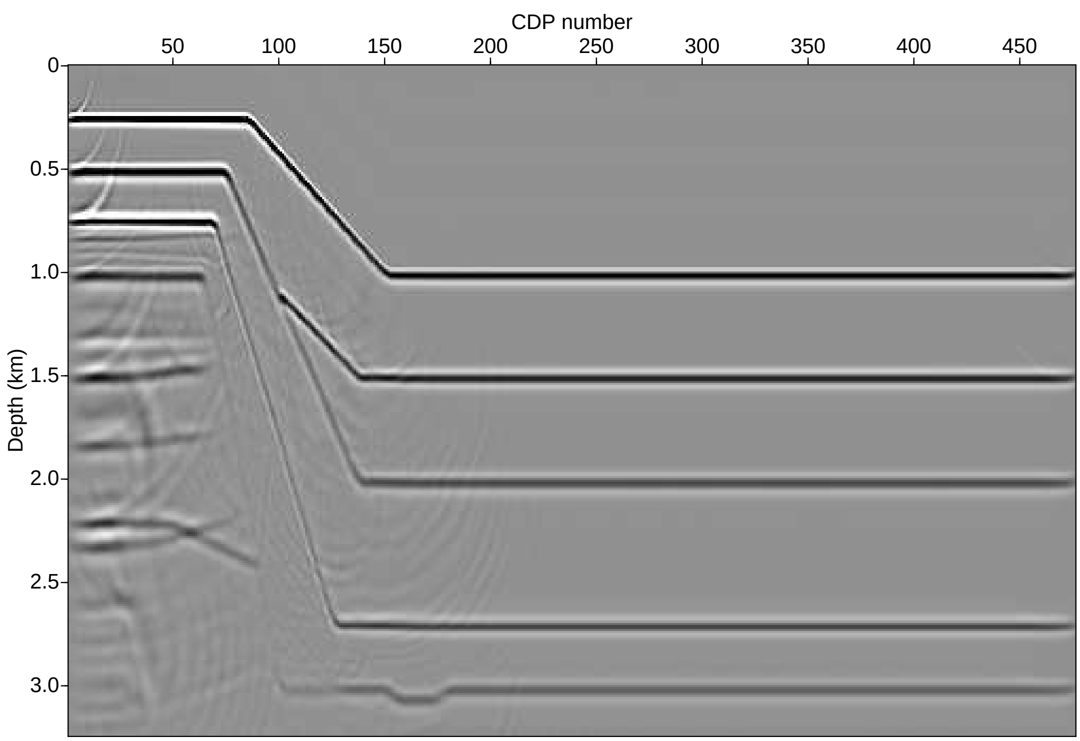

FIG. 6. Top: Section at $y = 0$ obtained with a 39-coefficient explicit extrapolator. Bottom: Same section obtained using GSP.

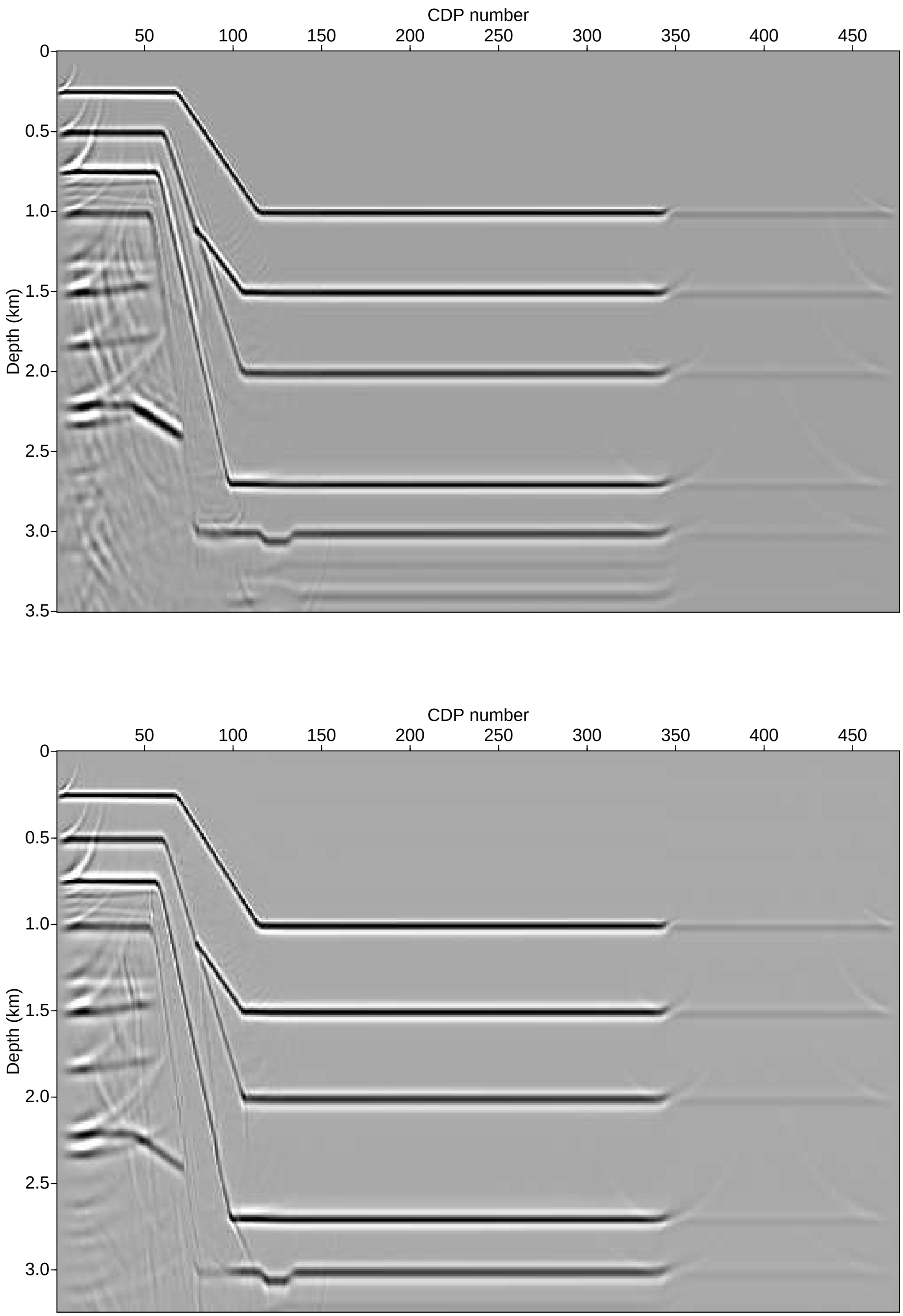

FIG. 7. Top: section along $x = y$ direction obtained with a 39-coefficient explicit extrapolator. Bottom: same section obtained using GSP.

where Δx represents the CMP in-line sampling interval. Using the Chebyshev recursion as in the case of the McClellan transform, the filter $\cos(n\Delta x k_s)$ can be written in terms of an n-th order polynomial of $\cos(\Delta x k_s)$. It remains to find the spatial stencil associated with the $\cos(\Delta x k_s)$ filter. To do so, we write:

$$\begin{aligned} G(k_{m_x}, k_{h_x}) &\equiv \cos\left[\Delta x\left(k_{m_x} - k_{h_x}\right)\right] \\ &= \cos\left(\Delta x k_{m_x}\right)\cos\left(\Delta x k_{h_x}\right) \\ &\quad + \sin\left(\Delta x k_{m_x}\right)\sin\left(\Delta x k_{h_x}\right) \end{aligned}$$

By inverse Fourier transform, we obtain:

$$g(m_x, h_x) = \begin{bmatrix} 0 & 0 & \frac{1}{2} \\ 0 & 0 & 0 \\ \frac{1}{2} & 0 & 0 \end{bmatrix}$$

The resulting convolution filter has only two nonzero entries, which makes it very inexpensive to apply. Note that the main anti-diagonal of the filter indeed represents the impulse response of the $\cos k_s$ filter, that is, the convolution is done in effect along the shot direction. Unequal sampling along the in-line offset and along the CMP in-line direction may be accomodated by methods similar to those developed for the zero-offset case [7].

We applied this explicit common-azimuth migration scheme to the SEG-EAGE salt model, and compared the results with those produced by the hybrid screen method. The data set was binned with a 20m CMP spacing in both the in-line and cross-line directions, and with 80m sampling along the in-line offset direction. Figure 6 (top panel) shows a typical in-line section through the velocity model, taken at constant cross-line coordinate $y = 9,820$m, while Figure 7 (top panel) shows a typical cross-line section through the velocity model, taken at constant in-line coordinate $x = 7,440$m. In each figure, the middle and bottom panels show the corresponding common-azimuth migrations results obtained via the hybrid screen method and via the explicit scheme, respectively. The results obtained with the explicit scheme are very satisfactory. More background noise is present, but the overall quality of the images obtained with both methods is very similar. In fact, the results obtained with the explicit method are surprisingly good, considering that the scheme was derived from the approximation with splitting of the common-azimuth dispersion relation.

CONCLUSIONS

We have presented an overview of 3-D depth-extrapolation methods and provided several comparisons with a well-tuned hybrid screen method. The tests we provided in this paper do support the widespread belief that explicit schemes are effective in handling strong velocity variations and can produce correct images of arbitrarily dipping reflectors. However, our results also suggest that these techniques require some fine tuning in order to reduce the frequency dispersion inherent to finite-difference schemes. We also presented a first attempt at migrating common-offset common-azimuth data with an explicit scheme. Preliminary results are encouraging and suggest that the technique be further investigated.

ACKNOWLEDGEMENTS

Special thanks go to my internship mentors Henri Calandra and Biaolong Hua for their guidance and support, to my advisor Bill Symes for many useful discussions, and to Jan Thorbecke for his kind assistance during various parts of the project.

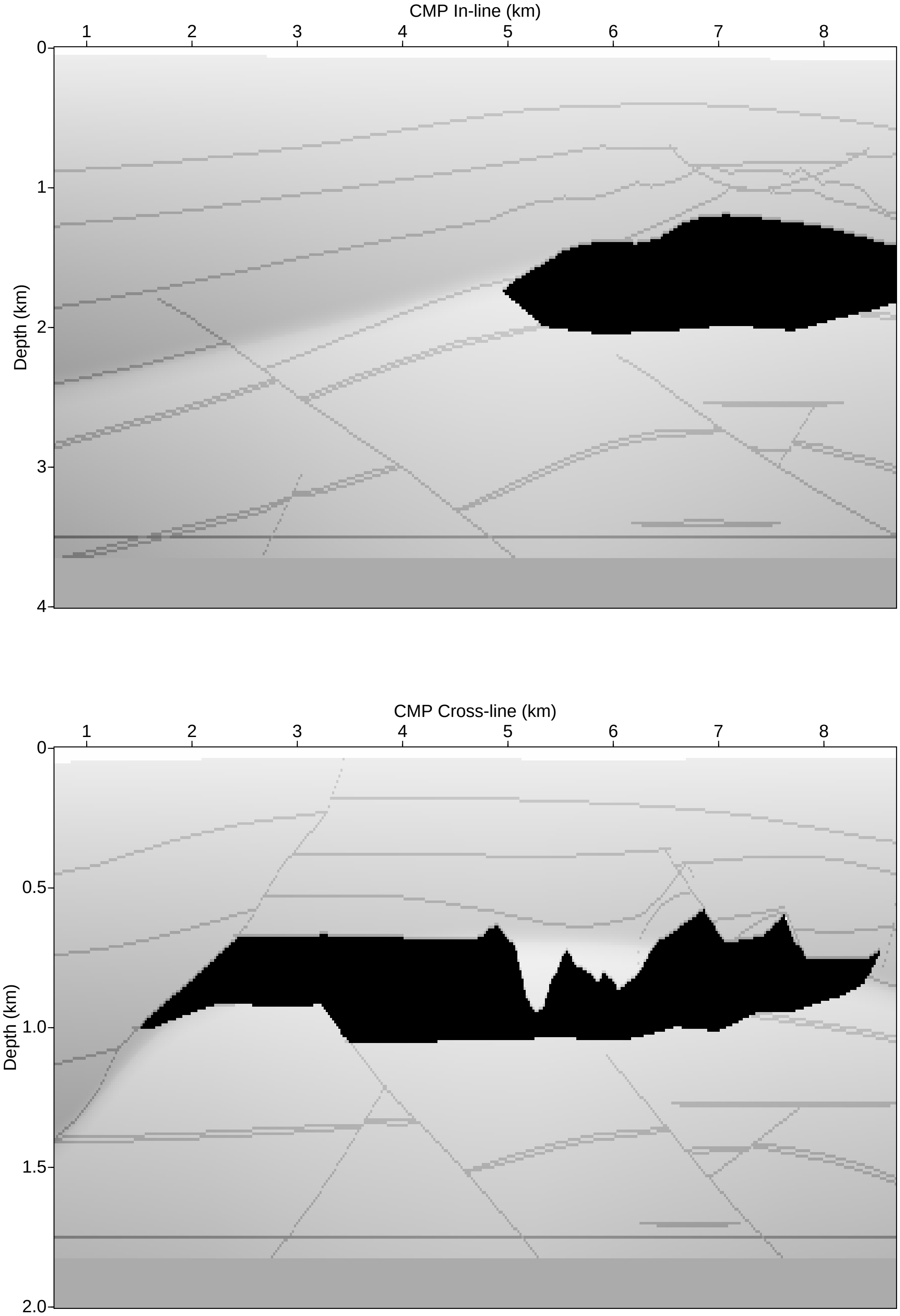

FIG. 8. Top: Velocity model at constant cross-line coordinate $y = 9,820m$.
Bottom: Velocity model at constant in-line coordinate $x = 7,440m$.

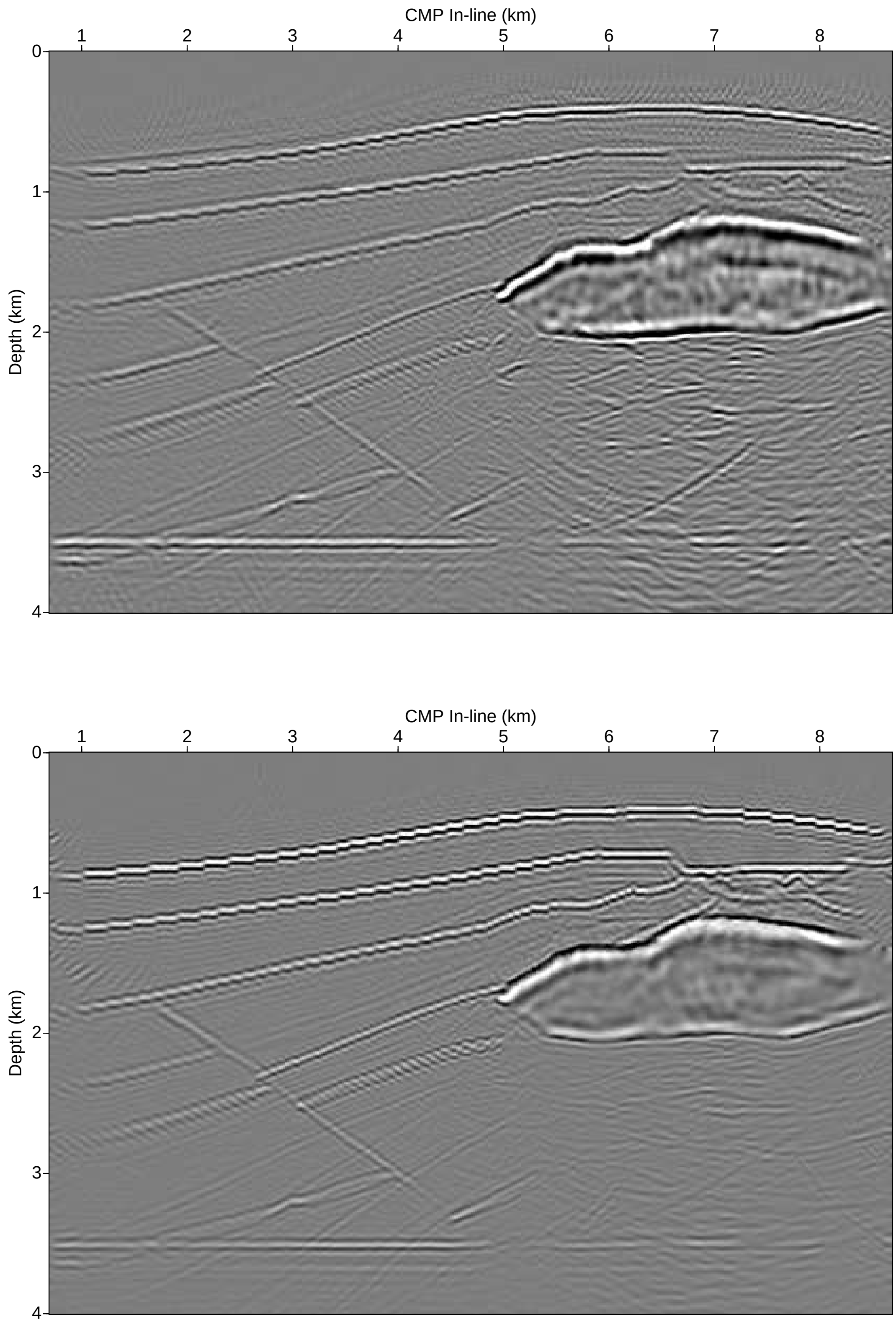

FIG. 9. Common azimuth migration at constant cross-line coordinate $y = 9,820m$:
Top: results obtained using the explicit method.
Bottom: results obtained using the hybrid screen propagator.

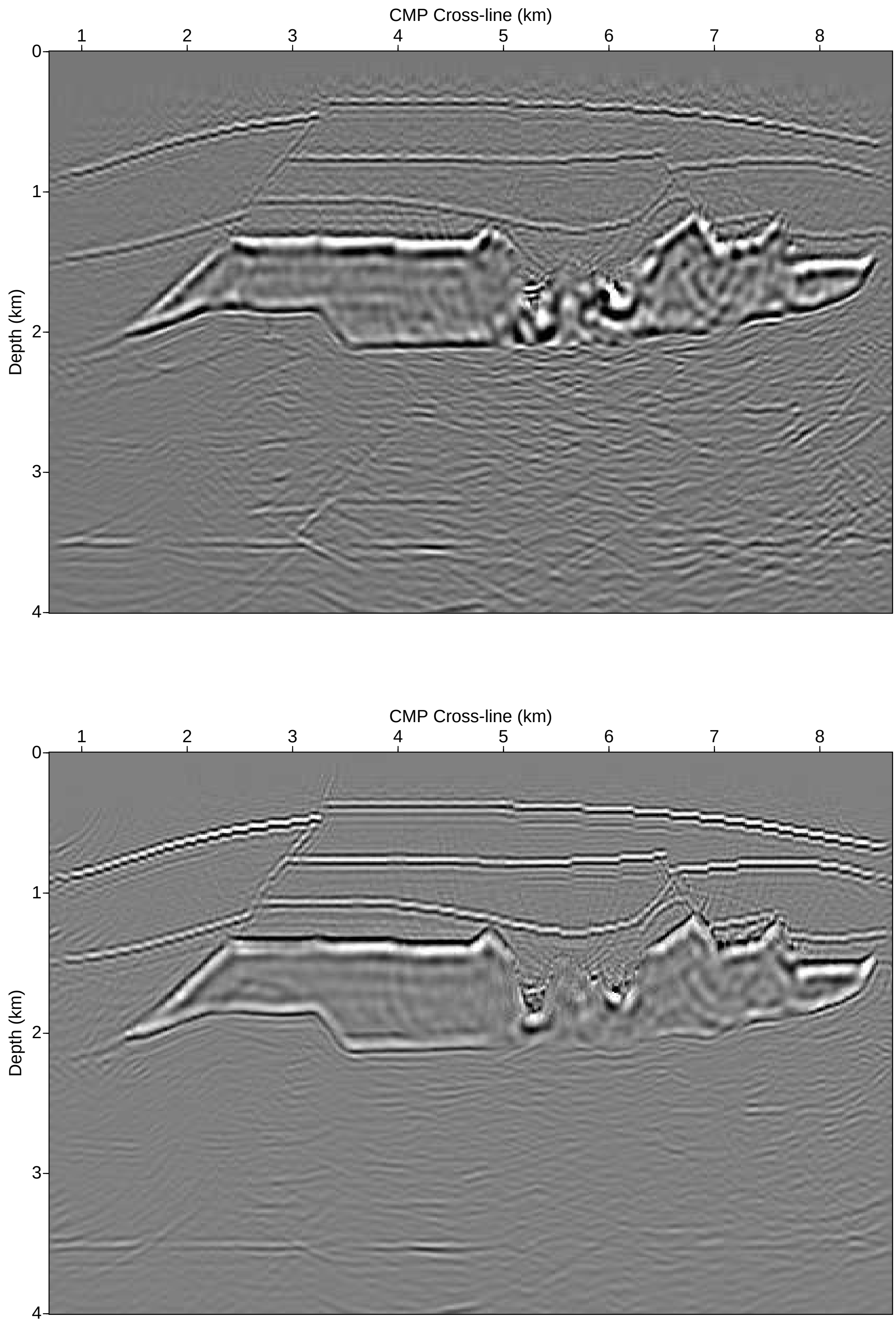

FIG. 10. Common azimuth migration at constant in-line coordinate $x = 7,440m$:
Top: results obtained using the explicit method.
Bottom: results obtained using the hybrid screen propagator.

REFERENCES

A. J. Berkhout. Wave field extrapolation techniques in seismic migration, a tutorial. *Geophysics*, 46:1638–1656, 1981.

B. Biondi and G. Palacharla. 3D depth migration by rotated McClellan filters. *Geophys. Prosp.*, 43:1005–1020, 1995.

B. Biondi and G. Palacharla. 3-D prestack migration of common-azimuth data. *Geophysics*, 61(6):1822–1832, 1996.

G. Blacquière. Optimized McClellan filters applied in one-pass 3D depth extrapolation. In *61nd Ann. Internat. Mtg.*, pages 1126–1129. Soc. of Expl. Geophys., 1991. Expanded Abstracts.

G. Blacquière, H.W.J. Debeye, C.P.A. Wapenaar, and A.J. Berkhout. 3D table-driven migration. *Geophys. Prosp.*, 37:925–958, 1989.

E. W. Cheney. *Introduction to Approximation Theory.* Chelsea, New-York, 1982.

Eric Dussaud. Downward continuation with explicit extrapolators and common azimuth migration. Technical report, Internship report, Total, 2004.

J.T. Etgen and D. Nichols. Application of the Li correction to explicit depth extrapolation methods. In *69th Ann. Internat. Mtg.*, pages 1366–1369. Soc. of Expl. Geophys., 1999. Expanded Abstracts.

J.E. Gaiser. Effective use of the Laplacian transformation for explicit finite difference 3D migration. In *64th Ann. Internat. Mtg.*, pages 1274–1277. Soc. of Expl. Geophys., 1994. Expanded Abstracts.

D. Hale. 3D depth migration via McClellan transformations. *Geophysics*, 56 (11):1778–1785, 1991.

D. Hale. Stable explicit depth migration of seismic wavefields. *Geophysics*, 56 (11):1770–1777, 1991.

S.N. Hazra and M.S. Reddy. Design of circularly symmetric low-pass two-dimensional FIR digital filters using transformation. *IEEE Trans. Circuits Syst.*, 33:1022–1026, 1986.

O. Holberg. Towards optimum one-way wave propagation. *Geophys. Prosp.*, 36:99–114, 1988.

S. Levin. $\Delta x \neq \Delta y$ in 3D depth migration via McClellan transformations. *Geophys. Prosp.*, 52:241–246, 2004.

Z. Li. Compensating finite-difference errors in 3D migration and modeling. *Geophysics*, 56(10):1650–1660, 1991.

J.H. McClellan and D.S. Chan. A 2D FIR filter structure derived from the Chebyshev recursion. *IEEE Trans. Circuits Syst.*, 24:372–378, 1977.

J.H. McClellan and T.W Parks. Equiripple approximation of fan filters. *Geophysics*, 37:573–583, 1972.

R. Mittet. Explicit 3D depth migration with a constrained operator. In *72nd Ann. Internat. Mtg.*, pages 1148–1151. Soc. of Expl. Geophys., 2002. Expanded Abstracts.

C.D.B. Notfors. Accurate and efficient explicit 3D migration. In *65th Ann. Internat. Mtg.*, pages 1224–1227. Soc. of Expl. Geophys., 1995. Expanded Abstracts.

M.S. Reddy and S.N. Hazra. Design of elliptically symmetric two-dimensional FIR filters using the McClellan transformation. *IEEE Trans. Circuits Syst.*, 34:196–198, 1987.

A. Sollid and B. Arntsen. Cost-effective 3D one-pass depth migration. *Geophys. Prosp.*, 42:755–776, 1994.

R. Soubaras. Explicit 3D migration using equiripple polynomial expansion and Laplacian synthesis. *Geophysics*, 61:1386–1393, 1996.

J.W. Thorbecke. *Common focus point technology.* PhD thesis, Delft University of Technology, 1997.

J.W. Thorbecke and A.J. Berkhout. 3-D recursive extrapolation operators: an overview. In *Expanded Abstracts, Soc. of Expl. Geophys., 64th Ann. Internat. Mtg.*, pages 1262–1265, Los Angeles, 1994. SEG.

J.W. Thorbecke and W.E.A. Rietveld. Optimum extrapolation operators – a comparison. In *EAGE Expanded Abstracts*, page P105, Vienna, 1994.

J.W. Thorbecke, K. Wapenaar, and G. Swinnen. Design of one-way wavefield extrapolation operators, using smooth functions in wlsq optimization. *Geophysics*, 69(4):1037–1045, 2004.

Y. Xie, C. Notfors, J. Sun, and Y. Zhang. Explicit 3D migration on rectangular bins. In *74th Ann. Internat. Mtg.,Soc. of Expl. Geophys.*, page MIG2.4, Denver, 2004.